

On the Local Form and Transitions of Symmetry Sets, Medial Axes, and Shocks

Peter J. Giblin
Department of Mathematics
University of Liverpool
Liverpool, England L69 3BX

Benjamin B. Kimia
Division of Engineering,
Brown University
Providence, RI 02912

Abstract

In this paper we explore the local geometry of the medial axis (MA) and shocks (SH), and their structural changes under deformations, by viewing these symmetries as subsets of the symmetry set (SS) and present two results. First, we establish that the local form of the medial axis must generically be one of three cases, which we denote by the A notation explained below (here, it merely serves as a reference to sections of the paper): endpoints (A_3), interior points (A_1^2), and junctions (A_1^3). The local form of shocks is a sub-classification of these points into six types. Second, we address the (classical) instabilities of the MA, i.e., abrupt changes in the representation with a slight changes in shape, as when a new branch appears with slight protrusion. The identification of these ‘transitions’ is clearly crucial in robust object recognition. We show that for the medial axis only two such instabilities are generically possible: (i) when four branches come together (A_1^4), and (ii) when a new branch grows out of an existing one (A_1A_3). Similarly, there are six cases of shock instabilities, derived as sub-classifications of the MA instabilities. We give an explicit example of a dent forming in an ellipse where many of the transitions described in the paper can be seen to appear.

1 Introduction

Symmetry-based representations are a useful representation of shape for object recognition, free-form shape design, animation, path planning, *etc.* Consider a planar region enclosed by a simple smooth curve, referred to as the ‘boundary curve’. Blum [2] defined the *Medial Axis* (MA) as the locus of centers of circles wholly inside the region which are bitangent—tangent to the boundary curve in more than one place—together with limit points of this locus. This has in turn led to other definitions of symmetry [13, 1] such as the mid-cord locus, mid-arc locus, and the (full) *symmetry set* (SS) [6] which is the locus of centers of *all* bitangent circles (together with limit points of this locus). Thus, the medial axis is a subset of the symmetry set. The *shock set* (SH) is a *dynamic* view of the MA where the propagation of waves (‘grassfire’) from the boundary leads to the formation of singularities which themselves propagate. With each point of the medial axis there is an associated *radius* r of the corresponding bitangent circle (or limit of such circles). The direction of increase of this radius function can be indicated on the medial axis by an arrow, and this gives the shock set. Endowing the medial axis in this way with a sense of flow, as was hinted to by Blum [2], leads to a finer partitioning of its branches at points where the flow reverses, thus generating a more discriminating hierarchy of qualitative structure which is at the same time perceptually more salient. See Figure 1.

We shall shortly introduce the A notation for contact of circles with curves. We avoid using the word ‘order’ to describe this contact since there is another ‘historical’ use of the word in connection with shocks. Here the ‘ k ’ in ‘ k^{th} order shock’ does not have a significance beyond simply listing the cases in *some* order. Specifically, first-order shocks are points where r does not have an extremum (‘monotonically flowing points’), second-order shocks are points of the MA where r has a local minimum, so that flow is outward in both directions (source of flow), and fourth-order shocks are MA

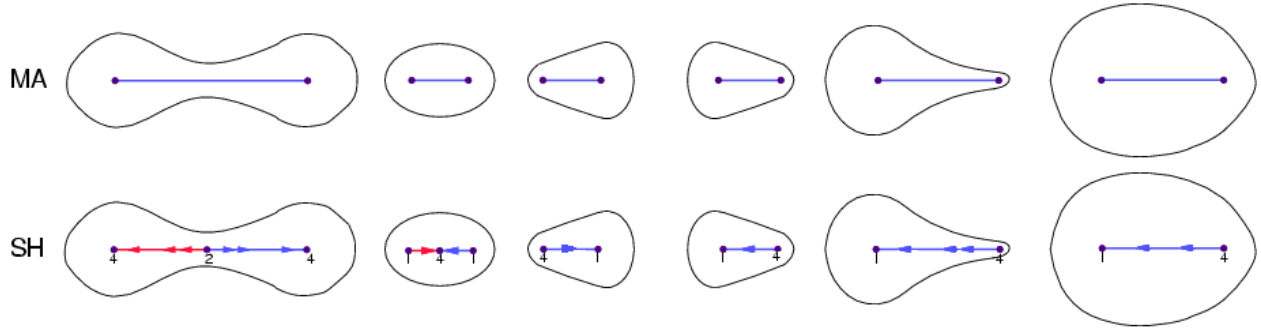


Figure 1: The shapes in the top row all have the same medial axis (MA), but the shock sets (SH) in the bottom row distinguishes between qualitative categories of shape even when the numerical information is stripped from it and only the shock graph topology is retained. Arrows indicate the direction of shock flow with double arrows indicating higher velocities.

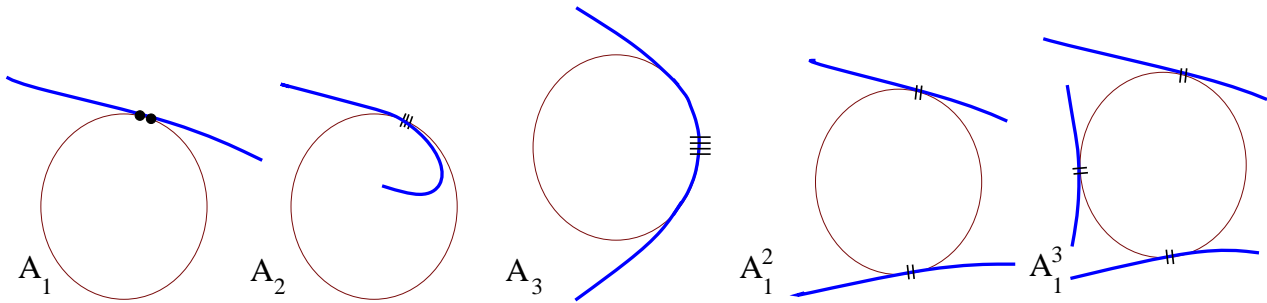


Figure 2: This figure illustrates the notation A_k^n in the context of the contacts of the curves (thick) with circles (thin) in 2D.

points where r has a local maximum so that the flow is inwards (sinks of flow). Third-order shocks are non-generic points with infinite velocities (simultaneously a source and a sink of flow): r is constant along a segment of the MA.

The practical use of these symmetry representations for recognition often relies on matching the qualitative structure of the shape, as captured by a tree or graph [23, 9, 16, 18, 21]. This requires an identification of special points and groups of points to be used as nodes and links of this graph. Thus, a classification of types of points that arise in symmetry-based representations and the nature of their local geometry is important to the construction of a graph. In addition, this classification of local form has been a basis for the *exact* recovery of the shock structure, see Section 5.

This classification of local form relies on the contact between a circle C and a curve γ , and we use notation due to V.I. Arnol'd (see for example [5]). A circle and curve are said to have A_k contact if they have $k + 1$ coincident intersection points. See Figure 2. Thus A_1 contact is ‘ordinary’ tangency—two coincident intersections—while A_2 contact means that the circle C passes through ‘three coincident points’ of the curve γ and so is the circle of curvature. Thus the radius of curvature of γ equals the radius of C at the tangency point. Next, A_3 contact means that C is the circle of curvature and has four coincident intersections with γ . This implies that C is the circle of curvature at a vertex (stationary point of curvature) of γ . By extension of this notation, a circle and curve have A_1A_1 or A_1^2 contact if they have ordinary tangency at two distinct points, A_1A_2 contact if there is ordinary

tangency at one point and C is the circle of curvature at another point, and so on. The symmetry set is the locus of centers of circles for which the contact is ‘at least as degenerate as A_1^2 ’, since this allows for the limit points mentioned in the definition.

The local form of the SS was established in [6]. Here, we use this to establish the local form of the medial axis and of the shock set, including a number of geometrical features of both. For a different approach to the medial axis, via minimum functions, see [3, 4]. For a topological classification of the ‘central set’ and cut focus which are related to the medial axis, see [22, 8]. Section 2 shows that the only generic possibilities for a medial axis point are those of a typical point of a branch, a junction (branching point) A_1^3 , and an end point A_3 ; other forms are not generic for a single curve, but can generically happen in a one-parameter family of deformations of a curve. The latter are addressed in Section 3. A configuration is called *generic* here if it cannot be avoided by arbitrarily small perturbations of the boundary curve. For example, if there is a circle with four ordinary tangencies (an A_1^4 circle) on a single curve γ then a small perturbation of γ will remove this configuration and leave only A_1^3 circles. But in a one-parameter family, an A_1^4 circle may momentarily appear (see the second row of Figure 21). Even if the family as a whole is perturbed slightly, there will still be some member which has an A_1^4 circle. On the other hand if a one-parameter family of curves exhibits an A_1^5 circle, then this phenomenon *can* be removed by a slight perturbation of the family.

First, in this paper we show the following.

Theorem 1 *The medial axis points are generically one of (i) end of a branch point (A_3), (ii) interior points of a branch (A_1^2), and (iii) the junction points of three branches (A_1^3). In addition, shock points can generically consist of three types of **sources**, namely, (i) end points A_3 with inward flow, (ii) interior points with outward flow A_1^2-2 (second-order shocks), and (iii) junctions of three branches with only one outward flowing branch A_1^3-1 , and of **sinks**, namely, (iv) interior points with inward flow A_1^2-4 (A_2 shocks) and (v) junction of three branches all of which are inward-flowing A_1^3-4 (A_3 shocks). All remaining points are first-order shocks connecting sources to sinks. Thus, the first five types of nodes and the sixth type, the first order shocks form links of a directed, planar graph (topological¹ shock graph).*

A second issue for the practical use of such a symmetry representation, *e.g.*, for recognition is the instability of the representation with slight changes in the shape. While typically small changes in shape cause small changes in the medial axis or the shock set, for shapes close to certain non-generic shapes small changes in shape cause abrupt changes in the MA or SH. The classic example of such an instability is that of a small protrusion in the shape which gives rise to a large branch of the medial axis, Figure 3 (top). A second example is caused by a slight shift in the location of one of the branches, Figure 3 (bottom). We call (sudden) structural changes of a skeleton a **transition**, and formally show that the transitions of Figure 3 are the only generic instabilities of the medial axis. These transitions each correspond to an edit operation in an edit distance approach to computing shape similarity, which makes shapes on either side of the transition equivalent [21, 12, 15].

Theorem 2 *Shapes varying under a generic one-parameter family of deformations can only depict two types of transitions: (i) two nearby junctions merge into a junction of four branches (A_1^4 ; see Section 3) and then two close by junctions with different arrangement of branches reappear, (ii) the growth of a new branch from an interior branch point (A_1A_3 ; Section 3). Similarly, consideration of velocity along each branch leads to six types of shock transitions identified by Figure 20.*

¹The complete shock graph is the topological shock graph together with geometry and dynamics of each branch.

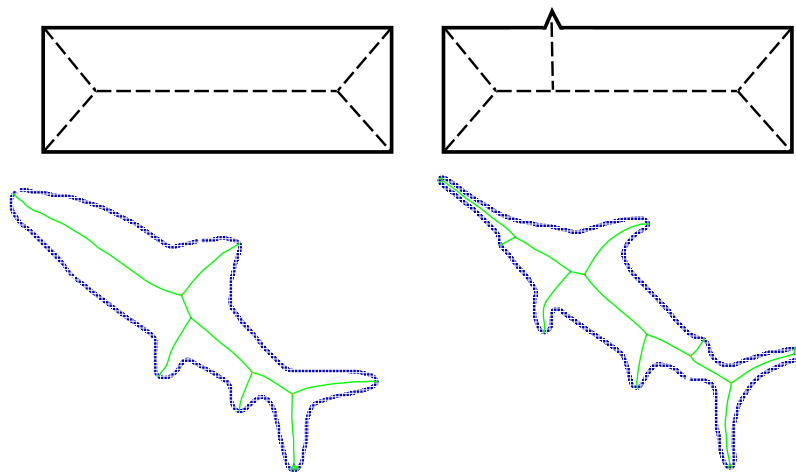


Figure 3: Two classic instabilities of the medial axis: (top) a small protrusion gives rise to an unproportionately large branch; (bottom) a small shift in the location of the lower fin of the fish drastically alters the graph structure of the skeleton, thereby causing difficulties for graph matching algorithms for object recognition. These are two of the transitions discussed later in the paper; see Figure 20 and 21.

The significance of Theorem 2 is in that (i) it assures that no other generic instabilities exist, and (ii) it suggests ‘edit operations’ which identify skeletons close to this instability on either side by identifying both with the non-generic skeleton itself, thus ensuring the equivalence of shapes on either side of the instability. The identification of instabilities and implementing regularizing measures are critical for robust recognition using skeletal graphs [21, 12, 14].

Although only the transitions noted above can occur on the medial axis, it is not true that other transitions occurring on the symmetry set are of no significance for the study of the medial axis. In fact we detail other transitions in the structure of the symmetry set which are essential in order that later events can occur on the medial axis. The growth of an extra branch of the medial axis is really prefigured by an ‘ A_4 transition’ which occurs on the symmetry set. The boundary curve has acquired two new stationary curvature points (vertices) which creates a new branch of the symmetry set. At a later time this may ‘penetrate’ the medial axis and create new structure there. This is shown happening in Section 4; see also Figure 12.

Another even more subtle symmetry set event is an ‘exchange of cusp branches’ which occurs with an A_2^2 transition. We give some details of this in Section 3 and an example where it can be observed happening in Section 4. The moral to be drawn from this is that although the symmetry set is not the object of prime interest, it is not possible to understand the evolution of the medial axis fully without seeing ‘behind the scenes’ to what is happening on the symmetry set.

2 The Local Form of Symmetries of Two Dimensional Shape

The local form of the symmetry set was derived in [6], as summarized in the top row in Figure 5. Thus the local forms are:

\mathbf{A}_1^2 : An ordinary smooth point of the symmetry set, where the bitangent circle has ordinary contact at two places on the curve;

\mathbf{A}_3 : An endpoint of the symmetry set, where the center of the circle is the center of curvature at a vertex (stationary point of curvature);

$\mathbf{A}_1\mathbf{A}_2$: A cusp on the symmetry set, where the center is the center of curvature at one of the tangency points;

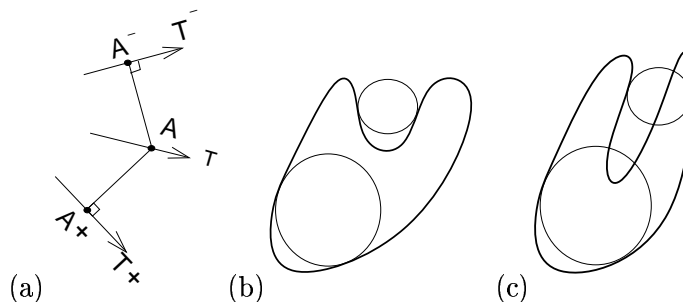


Figure 4: (a) The computation of a point A of the SS is locally dependent only on A^- and A^+ and their tangents. In contrast, the computation of the medial axis is global. An illustration of two bitangent circles that are maximal (b) and two that are not (c). Thus, not all points of the symmetry set belong to the medial axis.

$\mathbf{A}_1^2/\mathbf{A}_1^2$: (not important for our purposes): the symmetry set has a crossing which is the center of two circles of different radii both bitangent to the curve;

\mathbf{A}_1^3 : A triple crossing on the symmetry set, brought about by a circle tangent to the curve in three places.

However, the local form of the medial axis or of the shock set has not been derived thus far. We examine the local form of medial axes (MA) and shocks (SH) by observing that these symmetries are subsets of the symmetry set (SS). Specifically, each medial point or shock point is a symmetry point that satisfies not only the *local* bitangency requirement of the symmetry set, but also that the *global* condition that the bitangent circle is maximal. This means that the radius of the circle equals the (smallest) distance from the centre of the circle to the curve. See Figure 4.

It is a standard result about symmetry sets (see for example [6]) that the perpendicular bisector of the chord joining the two points of contact of a bitangent circle is *the tangent line* to the symmetry set. (This line certainly passes through the center of the circle, which is the symmetry set point.)

A shock point is a medial axis point with additional qualitative properties, and can thus be only one of $\{A_1^2, A_3, A_1^3\}$.

We now proceed with the proof of Theorem 1:

Proof: Since MA points are a subset of SS, we examine the viability of each of the five local forms of the SS for the MA and the SH:

(a) \mathbf{A}_1^2 : This is certainly a viable case for the medial axis, Figure 5(a). For the shock set, the velocity along this portion of the medial axis can generically be oriented either way corresponding to whether the radii of the bitangent circles are decreasing or increasing (1st order shocks), have a local minimum (2nd order shocks), a local maximum (4th order shocks), or be constant either on one or both sides (3rd order shocks), Figure 6(a). The latter is not generic for a single curve or a 1-parameter family.

(b) \mathbf{A}_3 : This local form of the symmetry set is also identical with the one for the medial axis provided the vertex is a maximum of curvature. For the shock description, however, note that the radius must be increasing away from the end point, Figure 6(b), and the opposite situation is not generically possible.

(c) $\mathbf{A}_1\mathbf{A}_2$: This means that A_1 and A_2 occur for the *same* circle. This case does not occur for the medial axis since A_2 implies a bitangent circle that crosses the shape. Consequently, this also does not occur for the shock set.

(d) $\mathbf{A}_1^2/\mathbf{A}_1^2$: This involves a point which is simultaneously A_1^2 for two separate pairs of tangents, *i.e.*

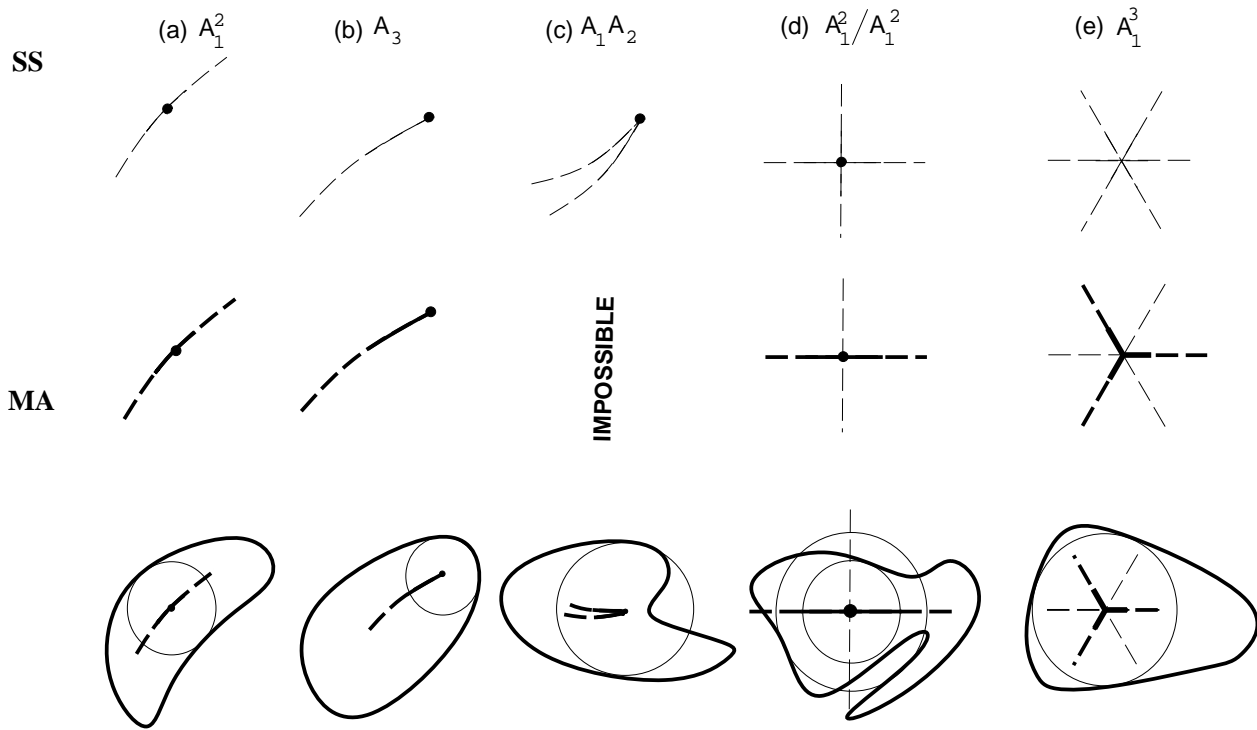


Figure 5: The top row illustrates the five local forms of the symmetry set, while the corresponding medial axis local forms are shown in the middle row. The bottom row depicts examples for each. Thin broken lines depict the SS while the thick broken lines depict MA points; solid thick lines depict the boundaries; bitangent circles are drawn in thin lines. (a) A regular segment of the symmetry set with ordinary bitangencies, *i.e.*, consisting of A_1^2 points. (b) The end point of a regular branch where the two points of tangencies overlap, *i.e.*, an A_3 point corresponding to a vertex on the boundary. (c) A cusp point connecting two branches, resulting in an A_1A_2 point. (d) A cross-over of two regular branches, but which each have different radii at the cross over point, *i.e.*, an A_1^2/A_1^2 point; the / indicating circles with different radii. (e) An intersection of three regular branches where the radii of the three branches are equal, *i.e.*, an A_1^3 point.

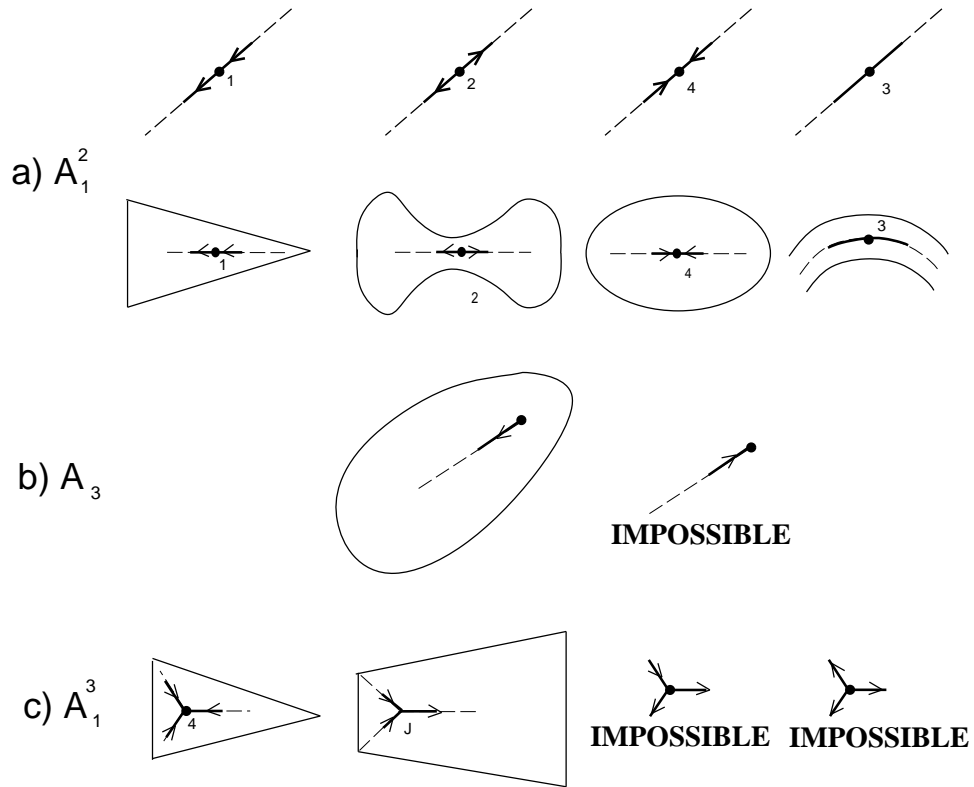


Figure 6: The three generic local forms of the medial axis, when augmented with the additional constraints of velocity, describe the generic local forms of shocks: (a) First, second, and fourth order shocks. The third-order shocks are not generic and are described for completeness. (b) The only form of A_3 is an outward velocity. Moreover $v = 1$ at these points. (c) Of the four combinatorial possibilities, only two configurations are possible: all branches move inwards, or, two inwards and one outwards.

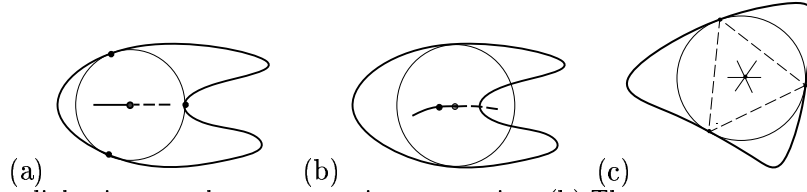


Figure 7: (a) The medial axis can only stop at a tritangent point. (b) The symmetry set continues beyond this point (c) A tritangent point generates $\binom{3}{2} = 3$ distinct symmetry set branches.

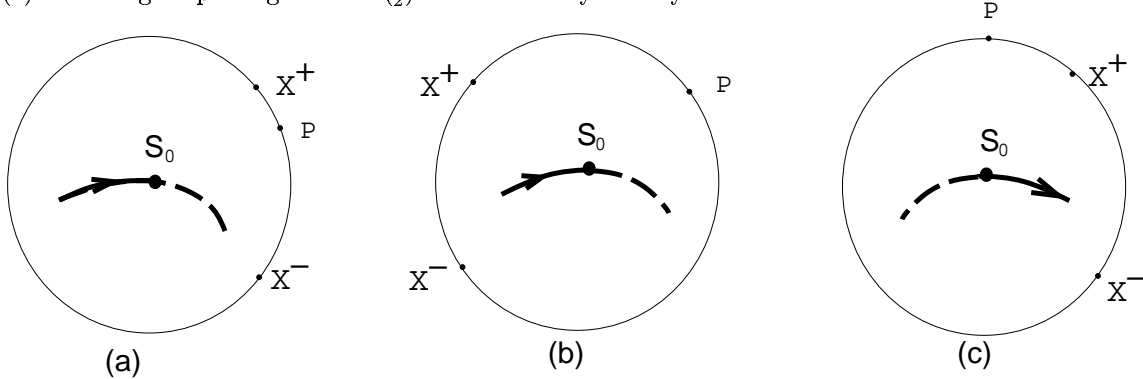


Figure 8: This figure illustrates that the position of the third point of tangency P with respect to X^+X^- determines which of the two sides of the symmetry set is visible as the medial axis and which is invisible. Let the symmetry set γ be oriented from left to right. (a) $(X^+ - P) \cdot T < 0$ so that for small $s > s_0$ we have $f(s) < 0$, which implies this branch is invisible. (b) Here also $(X^+ - P) \cdot T < 0$ and the same argument holds. (c) $(X^+ - P) \cdot T > 0$ the opposite argument holds. The medial axis is shown in solid lines while the symmetry set is shown in broken lines.

the point is the center of two distinct bitangent circles. Thus, only the branch of the SS with the smaller radius can be maximal and therefore be visible in the medial axis. Note that the two radii can be equal, resulting in an A_1^4 , *e.g.*, a square. While this case is not generic for one curve, it is a generic transition in a family of curves, *e.g.* rectangles approaching a square, Section 3.

(e) \mathbf{A}_1^3 : This is the only way the medial axis can cease to follow the symmetry set, *i.e.*, for the circles to become non-maximal. In other words, we must have another tangency point at the transitional moment, Figure 7. We now explore the configuration at A_1^3 points. ■

When there is a tritangent circle with all the tangencies being ordinary (2-point or A_1 contact), slight perturbation of any pair produces a series of bitangent circles the locus of whose centers gives rise to a symmetry branch. Thus, the symmetry set has three distinct branches through the center of the tritangent circle, corresponding to the three pairs of points which can be chosen from three points, Figure 8(c). The three tangents to these branches are perpendicular bisectors of the sides of the triangle of contact points. Consider the medial axis and symmetry set close to this situation, Figure 8(c). Suppose P is a third contact point of curve and the tritangent circle, X^+ and its reflection X^- in the tangent \vec{T} to the SS being the other two contact points.

Lemma 1 *Along each symmetry set branch the medial axis stops at A_1^3 points and the symmetry set continues in the direction of entering the arc of the circle containing the two characteristic points X^+ and X^- and the third contact point P .*

Proof: Consider the function $f(s) = \|\gamma(s) - P\|^2 - (r(s))^2$, where s is arc-length of the symmetry set branch $\gamma(s)$ and $r(s)$ is the radius of the bitangent circle. Let s_0 correspond to the A_1^3 point, with P

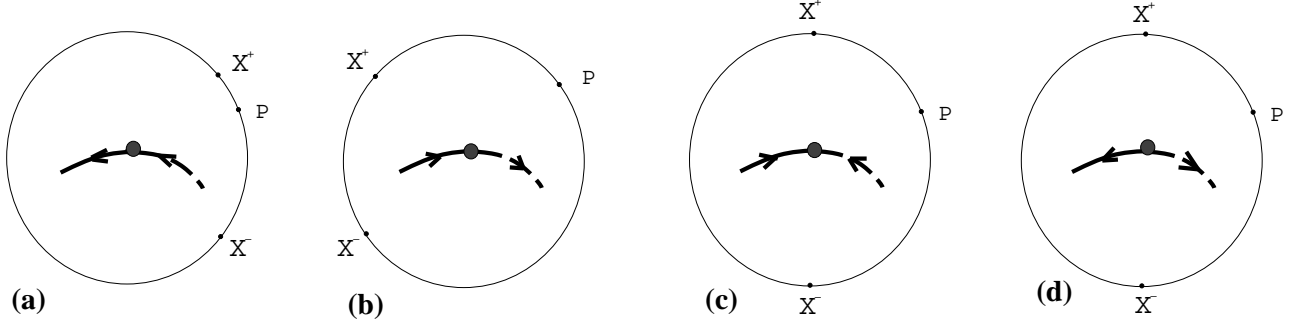


Figure 9: This figure illustrates the flow directions on the visible portions of the SS(MA). The three cases of (a) $r' < 0$, (b) $r' > 0$, (c) and (d) $r' = 0$. In the latter two cases which are only generic in a one-parameter family of deformations, the flow can be either inward or outward.

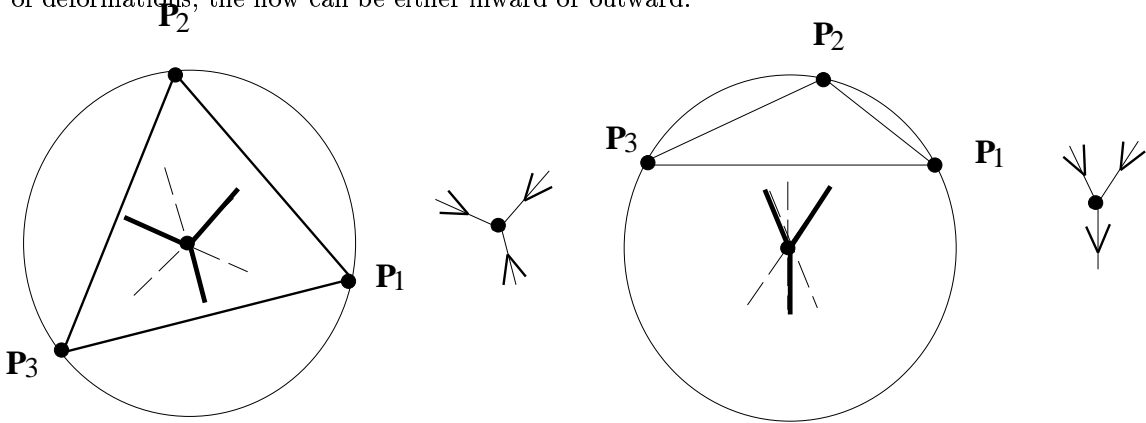


Figure 10: Each branch of the SS stops being part of the medial axis at A_1^3 point. These are the two possible generic configurations, depending on whether the center of the circle is inside or outside the triangle of contact points. (The case where the center is on the triangle creates a transition described in Section 3 as ‘ A_1^3 with infinite velocity’. See also Figure 9(d).)

denoting the third tangency point, and X^+ and X^- the characteristic points. Note that $f(s_0) = 0$. Now, if $f'(s_0) < 0$, then f is instantaneously decreasing at s_0 , which means, since $f(s_0) = 0$, that f is negative for small $s > s_0$. For such s , $\gamma(s)$ cannot be on the medial axis since the point P will have come inside the circle center $\gamma(s)$ radius $r(s)$. Now $f'(s) = 2(\gamma(s) - P) \cdot \vec{T}(s) - 2r(s)r'(s)$, so that $f'(s_0) < 0$ is equivalent to $(\gamma(s_0) - P) \cdot \vec{T}(s_0) < r(s_0)r'(s_0)$. We have $r(s_0)r'(s_0) = (\gamma(s_0) - X^\pm) \cdot \vec{T}(s_0)$. This in turn implies $(X^\pm - P) \cdot \vec{T}(s_0) < 0$.

The last condition is equivalent to one stated in the lemma, Figure 8, and completes the proof. Note that $(X^+ - P)$ cannot be perpendicular to $\vec{T}(s)$, since $P \neq X^-$. Thus, we can put an arrow on the SS/MA to indicate the direction in which r increases ($r' > 0$), Figure 9.

Lemma 2 *The three medial axis branches at an A_1^3 point are always obtained by taking every second one from the six symmetry set branches, that is the medial axis branches are ‘alternating’ among the symmetry set branches.*

Proof: In principle, only two combinatorial configurations can occur, namely, three adjacent MA branches, or an alternating series. However three adjacent MA segments must be contained in an angle of π . Take the three contact points at angles $0, \alpha, \beta$ round the circle ($0 < \alpha < \beta < 2\pi$) so that

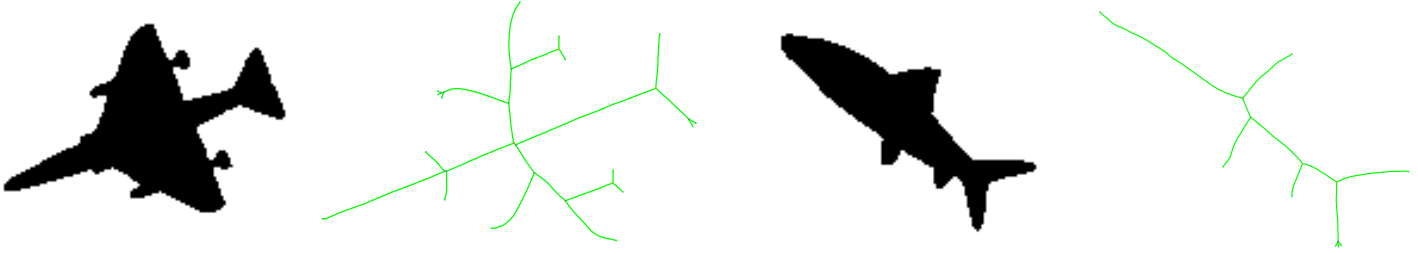


Figure 11: Two shapes (airplane and fish) and their associated shock graphs. The graph nodes are five types of shocks with first order A_1^2 's forming links.

the angles of the MA branches are $\frac{\alpha}{2}, \frac{\alpha+\beta}{2}$ and $\frac{\beta+2\pi}{2}$, respectively. Then, these can only be contained in an angle of π if either $\frac{\beta+2\pi}{2} - \frac{\alpha}{2} < \pi$, $\frac{\alpha}{2} + 2\pi - \frac{\alpha+\beta}{2} < \pi$, or $(2\pi - \frac{\beta+2\pi}{2}) + \frac{\alpha+\beta}{2} < \pi$, which lead to a contradiction. ■

Lemma 3 *The pattern of shocks at A_1^3 points is that of the medial axis with at least two branches with velocities flowing inward towards the A_1^3 point.*

Proof: There are potentially four combinatorial possibilities of the local flow, but only two are generically possible, Figure 10: Generically, P is inside the triangle $P_1P_2P_3$ or is outside of it. If P is inside, according to Figure 9, each of the MA branches must flow inward, Figure 10(a), a fourth order shock. If P is outside, accordingly two branches flow in and one flows out, Figure 10(b), a junction. ■

The Global Form: Global form arises by gluing together various local forms which can become adjacent. We have shown that the only ‘sources’ of shock flow are the A_1^3 with no outgoing branch ($A_1^3 - 4$), the A_1^2 which is a local max in radius and the A_1^3 with one outgoing branch ($A_1^3 - J$); the only “sinks” of shock flow are the A_3 , A_1^3 with an outgoing branch and the A_1^2 with a local maxima in radius (second-order shock). This is the formal proof of the shock grammar presented in [17]. The shock set can be described by an abstract graph, a directed planar graph, representing the topology of shock flow. Together with the shock geometry and dynamics, represented as attributes of the links, the graph leads to a complete reconstruction of the shape [10]. Figure 11 shows the shock graphs of two shapes arising from the classification of the local form.

3 Transition of Symmetries under Deformations

We now consider instability cases where skeletons change abruptly when the shape is altered only slightly. By regarding the SS and the evolute as together making up the ‘bifurcation set of the family of distance-squared functions’, the methods of singularity theory can be used to work out the structure of the SS in a generic one-parameter family of curves. There are quite a few cases, described in detail in the paper [7]. The local evolution of the symmetry sets is shown in Figure 12. All generic evolutions of symmetry sets can be analyzed into a sequence of local changes, and each change is one of the list.

However, some of these transitions are not immediately visible on the medial axis, in the sense that the center of the circle at the transitional moment cannot lie on the medial axis. In fact, only in the cases A_1^4 and A_1A_3 (see Figure 12) can the center be on the medial axis. Nevertheless, it is important to understand two other cases (A_4 and A_2^2 nib) because the event occurring there has a

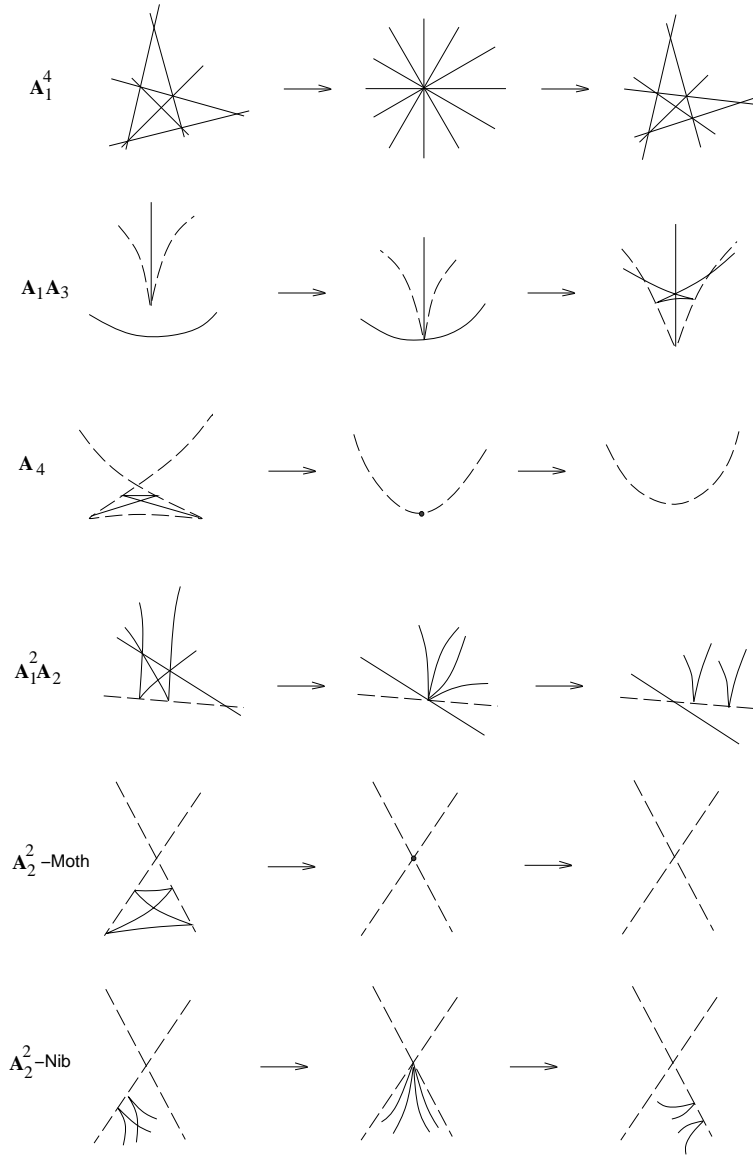


Figure 12: Transitions of the symmetry set occurring in a generic one-parameter family of curve deformations [7]. Transitions can occur either in the direction of the arrows, left to right, or in the reverse direction, right to left. *Note:* In this figure, the dashed line is the *evolute* (locus of centers of curvature) of the deforming curve, which is not shown. The medial axis will be a part of the symmetry set, and this part will never include the cusps on the symmetry set. The MA can come to an end only at endpoints of the symmetry set or at triple crossing points. Thus only A_1^4 and A_1A_3 can actually occur on the medial axis, but A_4 and A_2^2 ‘nib’ transitions on the symmetry set can have later repercussions for the medial axis (see text).

strong significance for the future evolution of the medial axis. The remaining two cases of Figure 12, $A_1^2A_2$ and A_2^2 moth, do not affect the medial axis—the creation of cusps by the latter transition is not significant until these cusps interact with others at a later time via an A_2^2 nib transition. The ‘nib’ has the subtlest effect of any of the transitions, and in fact we did not appreciate its crucial role until we examined the example discussed in Section 4. Because the cusps come together with a common tangent at the transitional moment of the ‘nib’, they are able to exchange branches and this is important for later developments of the medial axis.

We take the events of Figure 12 in turn.

A₁⁴ A circle is tangent to the boundary curve in four distinct points, all tangencies being ordinary. This is visible on the MA provided the circle is maximal.

A₁A₃ This is a crucial evolution since it is the *only* way in which new structure immediately appears on the medial axis. It occurs when a circle of curvature at a vertex of the boundary curve is tangent to this curve elsewhere. A formerly invisible branch of the MA with an endpoint becomes visible as it penetrates an existing smooth branch of the MA, emerging as part of a triple junction of MA branches. An example is in Section 4.

A₄ This occurs when the boundary curve acquires a ‘degenerate vertex’, which is the moment of birth (or death) of two ordinary vertices, one a maximum and the other a minimum of curvature. This is never visible on the MA since a circle with A_4 contact has 5 coincident contact points with the boundary curve and therefore (5 being odd) must cross the boundary curve. This prevents the circle from being maximal. However, in this evolution two new endpoints of the SS, one corresponding to the maximum and the other for the minimum curvature, are created and these can *later* interact with other parts of the MA, via an A_1A_3 transition, to become visible. So we have to consider this case. An example where it can be seen in action is in Section 4.

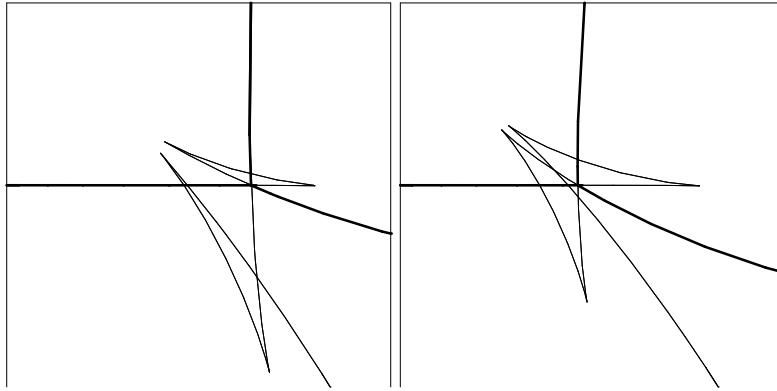


Figure 13: A ‘nib’ transition where two cusps on the symmetry set ‘change partners’. The heavy line is the medial axis. Note that although the cusps are not (can never be) on the medial axis, the change of partners is crucial for the later development of the medial axis. This is illustrated in Section 4.

A₁²A₂ In this case there is a circle which is osculating at one point (giving the A_2) and tangent at two others. An A_2 circle is never maximal (having 3-point contact with the boundary curve) and this transition involves only the loss (or gain) of triple crossings on the SS which are not part of the MA. No branches of the SS with endpoints are created which could later interact with the existing MA, nor do the cusps involved change branches (as happens with the next transition); therefore this transition does not by itself have an effect on the evolution of the MA, or SH.

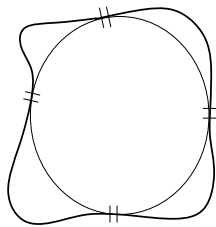


Figure 14: An A_1^4 point with a maximal bitangent circle is visible on the MA.

A_2^2 In this transition, there is momentarily a circle which is osculating (3-point, or A_2 contact) at two points of the boundary curve. At the moment of transition the circle cannot be maximal because the odd point contact necessarily makes it cross the curve. There are two versions of the transition, the so-called ‘moth’ and ‘nib’. In the first of these, cusps are created on the SS, but no structure, namely end-points as in the A_4 transition, which could later become visible. However, the ‘nib’ version turns out to be important for a most unexpected reason. Here, two cusps on the symmetry set interact in the manner of Figure 13. Four cusp branches before the interaction appear in the order 1, 2, 3, 4 say, with 1 and 2 paired, and 3 and 4 paired. But after the interaction 1 and 3 are paired and 2 and 4 are paired. This turns out to be crucial in that it allows a branch of the medial axis to ‘break free’ and eventually drift away. We illustrate this in Section 4 below.

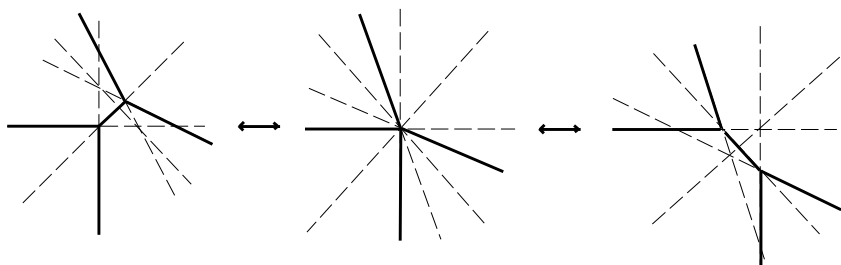


Figure 15: In these ‘before’ and ‘after’ diagrams showing the A_1^4 transition, dashed lines are ‘invisible’ symmetry set branches (that is, not on the medial axis) and solid lines are medial axis branches. The center diagram is the transitional moment itself. Note that on either side of this, one of the two invisible symmetry set branches supports a short piece of the medial axis while the other remains invisible.

We now consider three of the above transitions in more detail.

A_1^4 transition: This occurs in a family of curves when, momentarily, a circle is tangent at four points to one of the curves. Suppose that in fact this occurs for a circle which is maximal, so that its center belongs to the MA, Figure 14. The SS has six branches through the center of this circle, corresponding to the 6 ways you can choose 2 points from among 4.

Their tangents are along the perpendicular bisectors of the chords joining 2 of the 4 points. The first thing to note is that opposite pairs cannot contribute to the MA. For using the criterion in Section 2 both directions are barred for the MA, starting from the center of the A_1^4 circle. Each of the four pairs—given by taking consecutive pairs among the four contact points—will contribute a branch to the MA. The four MA tangents cannot all lie within an angle of π : suppose that the four contact points are at angles, 0, α , β , and, γ where $0 < \alpha < \beta < \gamma < 2\pi$. Then the medial axis tangent directions

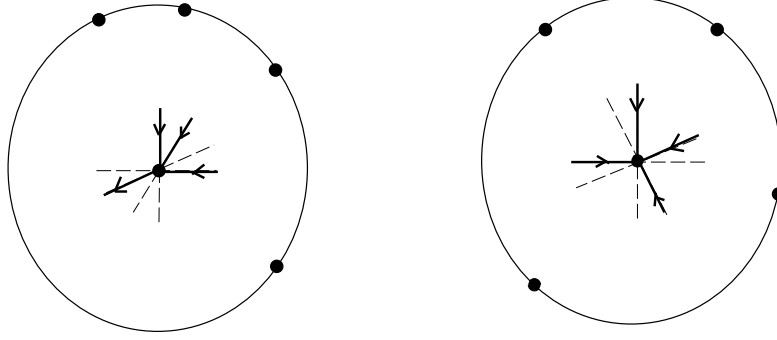


Figure 16: (left) All 4 characteristic points corresponding to an A_1^4 are in a semi-circle; all except one flow in. (right) The points are not on a semi-circle and all shocks flow in.

are $\frac{\alpha}{2}$, $\frac{\alpha+\beta}{2}$, $\frac{\beta+\gamma}{2}$, $\frac{\gamma+2\pi}{2}$. These can only lie within an angle of π if $\frac{\gamma+2\pi}{2} - \frac{\alpha}{2} < \pi$, $\frac{\alpha}{2} + 2\pi - \frac{\alpha+\beta}{2} < \pi$, $\frac{\alpha+\beta}{2} + 2\pi - \frac{\beta+\gamma}{2} < \pi$, or, $\frac{\beta+\gamma}{2} + 2\pi - \frac{\gamma+2\pi}{2} < \pi$. These give $\gamma < \alpha$, $\beta > 2\pi$, $\gamma - \alpha > 2\pi$, and $\beta < 0$, respectively, a contradiction. Since it is impossible for the ‘visible’ and the ‘invisible’ portions of the SS to alternate when there are four lines through a point, the following holds:

Lemma 4 *The four branches of the MA must be of the pattern shown in the center of Figure 15.*

It remains to describe the way in which the MA (and the SS) break up on either side of the A_1^4 transition. It is shown in the paper [7] that the only way the SS can evolve at an A_1^4 transition is shown in Figure 12. Detailed calculation proves that the passage through the A_1^4 singularity produces the transition of the medial axis depicted in Figure 15.

We now focus on the A_1^4 transition for shocks. The pattern of arrows, indicating increasing r or flow of the shocks, depends on the details of the configuration of 4 points on a circle. Figure 16 shows two examples at the A_1^4 configuration. An outward pointing arrow can only occur when the arc between two contact points, not containing other contact points is greater than π . Clearly, there can be only one such arc, so only one outward-pointing arrow is possible. If the angle is exactly π (a non-generic event here) then we need to know more information to determine the arrows. Of course, diametrically opposite points means $r' = 0$.

When all 4 arrows point inwards the pattern of arrows ‘before’ and ‘after’ will be as in Figure 17(a), where the arrows on the short segments can point either way. However, when one arrow points outside, this restricts the possibilities so that additional information is required to establish the flow which is in either case one of the two possibilities depicted in Figure 16. The arrows on the short segments can only point as shown to avoid conflict with the allowable triple crossing configurations of arrows, Figure 17(b).

A_1A_3 transition: This occurs in a family of curves when momentarily the circle of curvature at a vertex is tangent elsewhere, Figure 18. The MA (shown as a solid line) and rest of the SS (shown dashed) at this transitional moment has the configuration shown in Figure 18(a), when the point is itself on the MA. Note that the SS branch with an endpoint, before or at the moment when the collision occurs, cannot be part of the MA. Figure 18(b) shows the formation of a triple crossing where the SS pierces through and creates a short spur of MA, the evolute in the last picture is shown as well. The cusps on the SS as always signify A_1A_2 contact and are never part of the MA. The arrow shows r increasing.

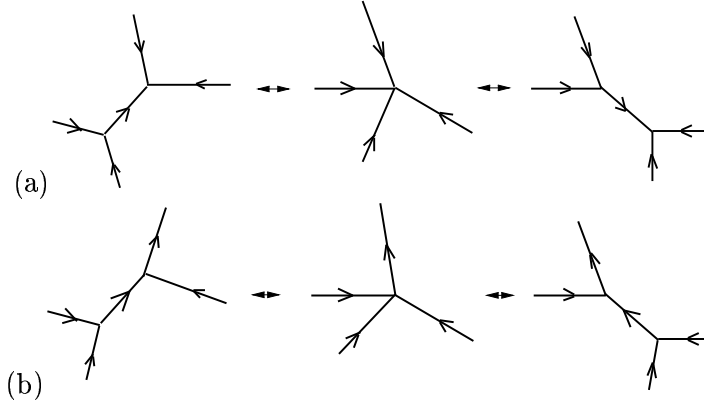


Figure 17: The A_1^4 transition for shocks. (a) This case is clearly symmetrical, the short central segments can carry arrows either way. (b) But this one isn't, you can't reverse these arrows because it violates the rule for triple intersections.

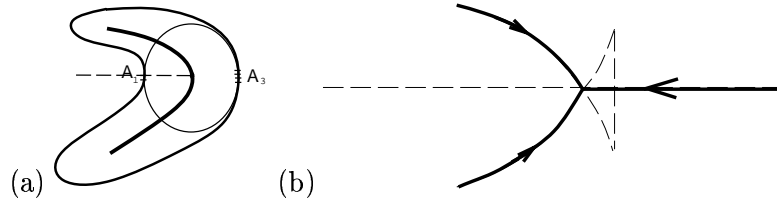


Figure 18: (a) The moment of A_1A_3 transition: the circle of curvature at a vertex (A_3) is tangent at another point (A_1). The apparently smooth branch of the medial axis (heavy line) actually has a singularity like $x = y^{4/3}$ at the point of intersection with the (dashed) symmetry set branch. (b) The dashed (invisible) branch pierces through and becomes visible as the shape is widened between the A_1 and A_3 points in (a).

It is worth pausing a moment to consider the phenomenon of a branch of the SS piercing another one. It is possible for this to happen in such a way that the two circles, one corresponding to the endpoint of the piercing branch, and the other corresponding to the point of the other branch where piercing takes place, to have *different radii*. In that case even though they have the same center there is no transition taking place, the pierced branch remains smooth throughout and nothing can change on the MA, as in Figure 22, bottom row. What we are dealing with above is the *generic* phenomenon of an A_1A_3 transition, where the two circles coincide, there is a transition on the SS, and will also be one on the MA if the smooth branch is in fact part of the MA. Watching the SS evolve there is not necessarily any way of telling whether there will be a transition when one piece with an endpoint pierces another piece. It all depends on whether the point where piercing occurs represents two circles with the same center but different radii, or one circle. Both events occur in the example of Section 4; see Figure 22.

It is also possible to imagine the symmetry set evolving in such a way that two smooth branches of it simply collide—this would mean that at the moment of collision they were tangential. But if this happens and there is a single circle centered at the collision point, rather than two concentric circles, then this circle is tangent to the boundary curve in four places. (The tangency of the two SS branches does not reduce this to three places.) This means that what is actually happening is the more complex

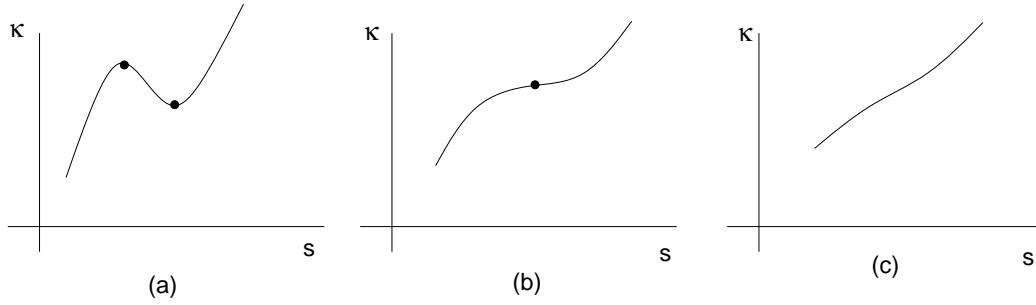


Figure 19: The curvature function close to an A_4 transition: (a) two extrema A_3 , merging (b) into one degenerate extremum A_4 where $\kappa' = \kappa'' = 0$, and (c) disappearing. This corresponds to the left-to-right sequence labeled A_4 in Figure 12, where the structure inside the ‘swallowtail’ disappears as the two A_3 points, corresponding to endpoints of the symmetry set, merge and disappear. The sequence (c) \rightarrow (b) \rightarrow (a) also occurs. Note that dashed lines in Figure 12 refer to the evolute.

A_1^4 transition, described above. It is not possible for two branches of the SS to cross, giving a single circle, without there being in fact at least one other branch of the SS through the crossing point.

A_4 transition: In this transition, two vertices—a local maximum and a local minimum of curvature—have just appeared, or disappeared, as the curve evolves in shape. So the curvature evolves as shown in Figure 19, either left to right or right to left. Note that no inflexions of the boundary curve (where the curvature function crosses the $\kappa = 0$ line) need be created at the same time.

The A_4 transition is invisible when it happens, but because, when running right-to-left in Figure 12, it produces two new end-points of the SS (it is the sole transition of the SS which does this), there is the possibility that at some later time one of these will penetrate a nonsingular branch of the MA and create a new ‘spike’ on the MA via an A_1A_3 transition. This occurs when creating a bump or an indentation; see the top row of Figure 22 and Section 4.

In addition to the transition inherited from the medial axis, the shock set has transitions related to conditions on the dynamics, namely, on velocity and acceleration, leading to two additional transitions, described below.

A_1^3 with infinite velocity: In this transition the initial velocity of a branch at a generic A_1^3 point (junction or 4th order shock) becomes infinite. The condition of infinite velocity, where the boundaries at the appropriate characteristic points are parallel, creates a transition since it can lead to two opposite flows with slight changes in the shape. In Figure 20(d) and (e) represent two possible transitions of this type. Figure 20(d) a second order shock approaches a 4th order A_1^3 which after the transition becomes a junction point. In Figure 20(e) a 4th order shock approaches a junction point and transforms it to a 4th order A_1^3 after the transition.

A_1^2 with infinite velocity and zero acceleration: In this transition, a second or fourth-order shock A_1^2 point (infinite velocity) approaches a fourth or second order A_1^2 shock, respectively. At the moment of collision, the A_1^2 point must have infinite velocity but zero acceleration, Figure 20(f). Figure 21 illustrate example shape deformations for each each transition in Figure 20.

4 An example: the dent

In this section we shall consider an evolving shape where the underlying structure of the symmetry set has a profound influence on the developing medial axis. It will illustrate several of the phenomena

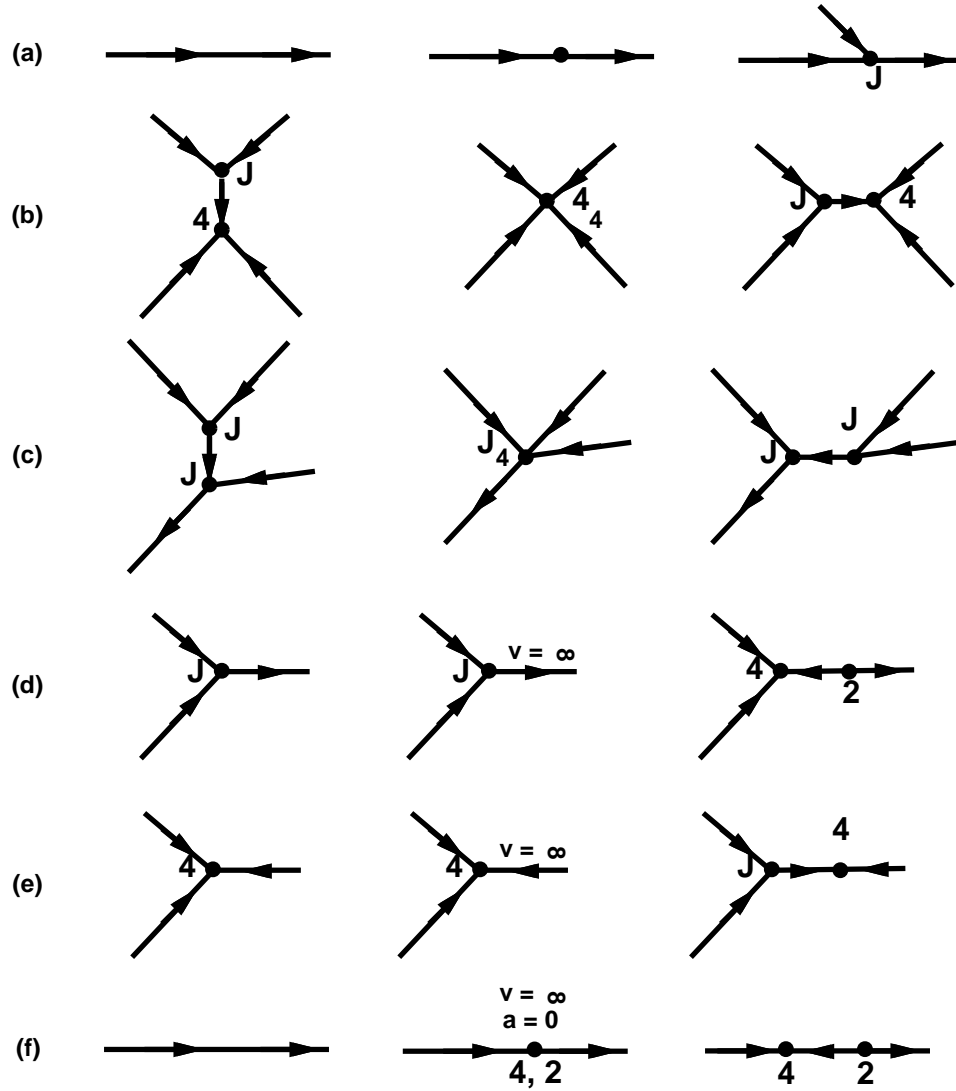


Figure 20: A schematic description of the transitions of shock structure. (a) is the A_1A_3 transition, (b) and (c) are the two types of A_1^4 , (d) and (e) are the two types of A_1^3 with infinite velocity, and (f) is the A_1^2 point with infinite velocity and zero acceleration.

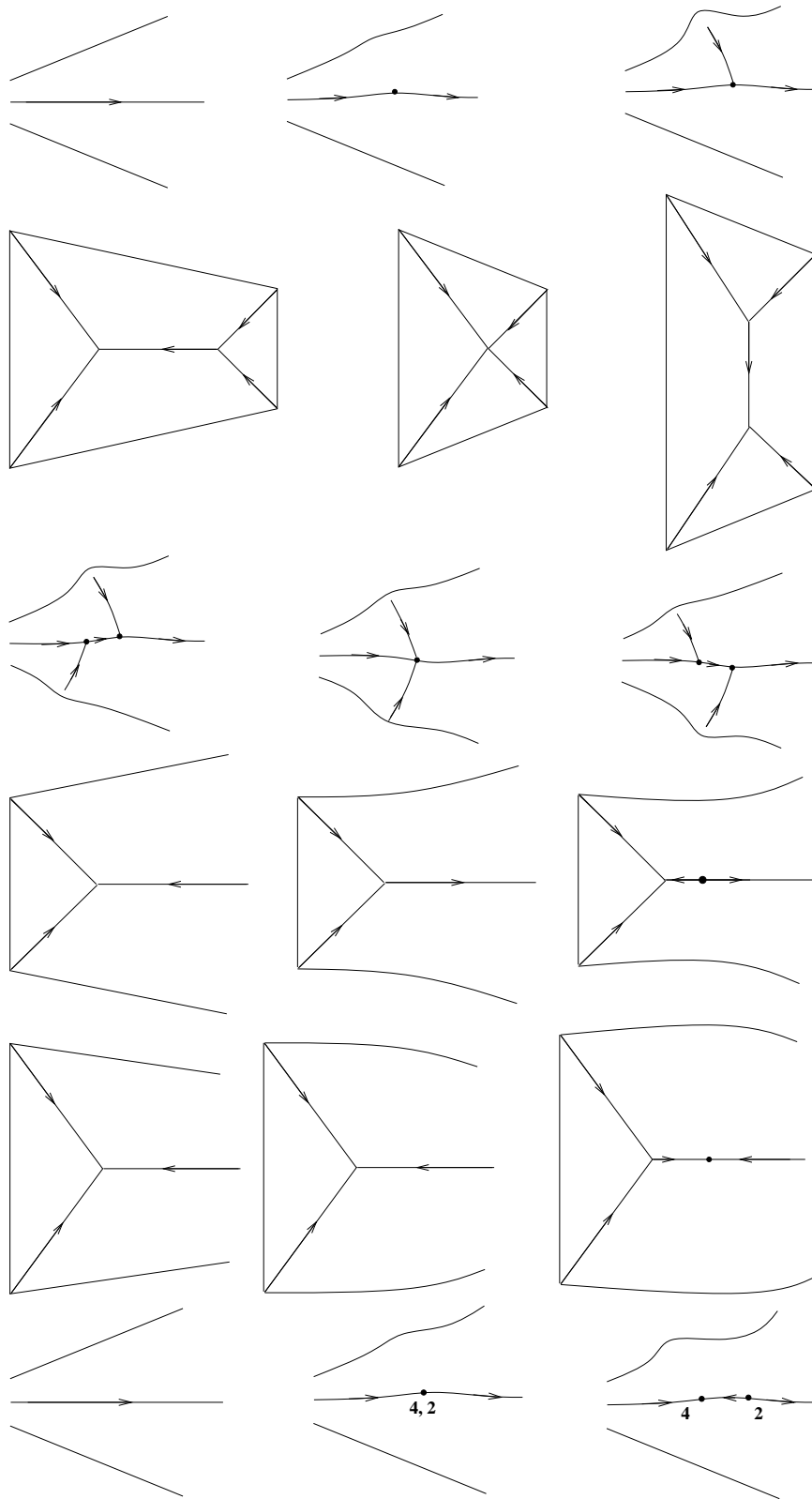


Figure 21: This figure illustrates examples of boundary deformations where the transitions in Figure 20 may occur.

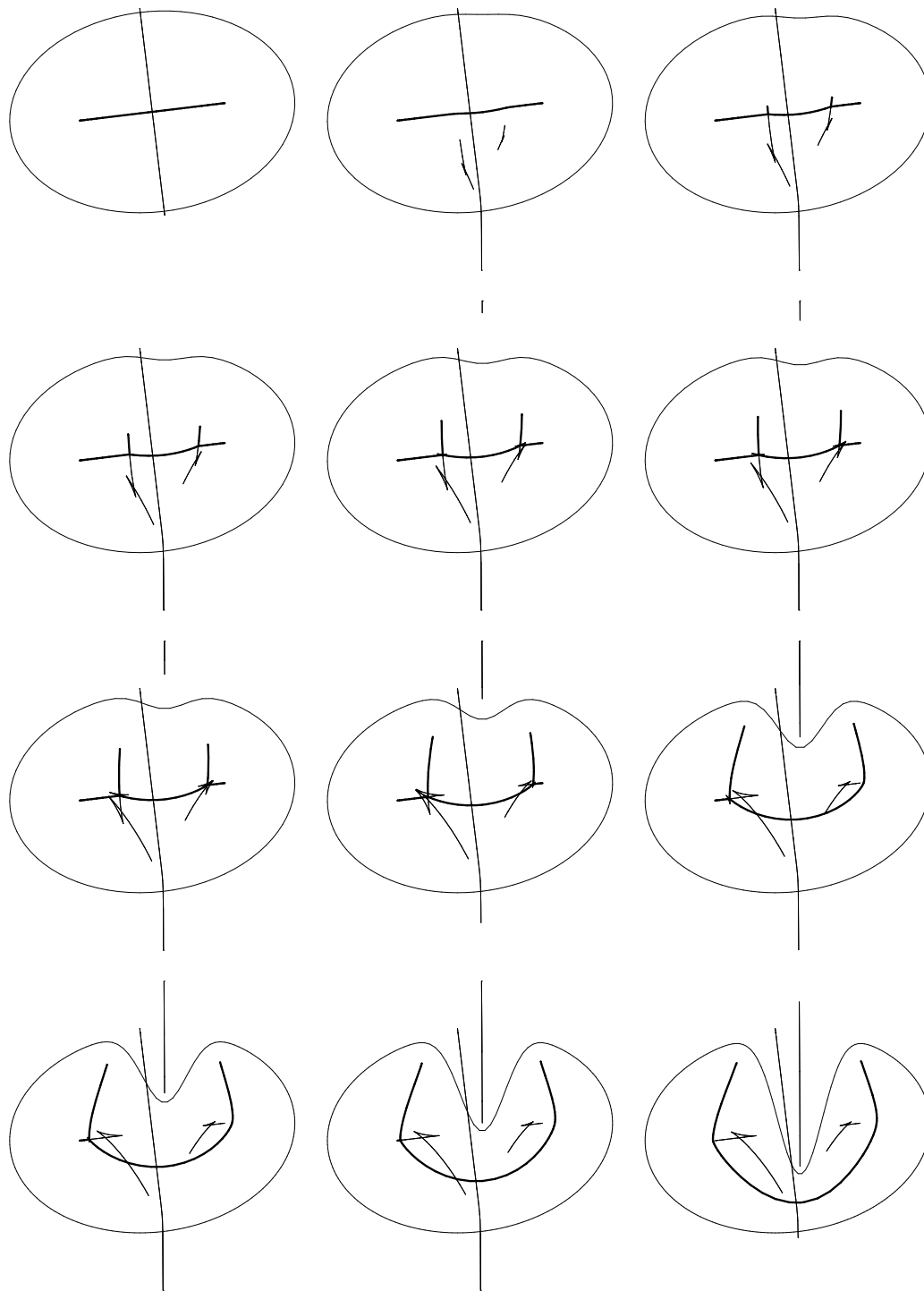


Figure 22: An evolving dent in an ellipse, the medial axis being the heavy line. The nearly vertical segment becoming evident in the bottom two rows, pointing into the dent from outside, is also part of the medial axis, but we are concentrating here on the interior part. For a commentary, see text.



Figure 23: A closeup of parts of Figure 22, namely the first two parts of the second row. In each case the concentration is on the events which are right of center. Left: note that where the symmetry set has pierced the medial axis (an A_1A_3 transition occurred just before this snapshot) there is actually a triple crossing (A_1^3) of the symmetry set Compare Figures 12 and 18. Right: a moment later: the two cusps are about to collide in an A_2^2 ‘moth’ transition whose function is to exchange cusp branches and allow one branch of the medial axis to ‘float away’, as in the last row of Figure 12. A closeup of a ‘nib’ transition, showing both before and after, is in Figure 13.

found above. The sequence of events is shown in Figure 22; here is a commentary.

An ellipse has symmetry set consisting of two perpendicular lines, the shorter one being the medial axis. (The other line is the locus of centers of circles tangent *externally* to the ellipse.) The ellipse in Figure 12 has semi-axes 2 and 1.4 long. A dent is introduced at the top of the ellipse, about 10° from the end of the minor axis. The dent is formed by subtracting $H \exp(-20u^2)$ from the y coordinate, u being the deviation of the angular coordinate on the ellipse from the birthplace of the dent. The parameter H is positive and varies in the whole Figure 22 from 0 to 2.

First row By the center diagram, two A_4 events have taken place, at slightly different times, yielding two new symmetry set branches. Compare the A_4 line (solid curve) of Figure 12 (where birth takes place right to left). By the end of the first row both new branches have penetrated the medial axis in separate A_1A_3 events, causing the appearance of two short segments of medial axis. Compare Figure 18.

Second row The new branches of the medial axis grow longer and by the end of the row an A_2^2 ‘nib’ event is taking place. See Figure 23 for an enlargement of the action to the right of center, and Figure 13 for another depiction of the nib event.

Third row Another nib event is taking place, this time left of center. The key feature of these events is that they enable branches of the symmetry set to detach themselves and drift away. This is happening right of center by the end of this row. As the symmetry set branch breaks clear, a right-pointing branch of the medial axis shrinks and disappears, leaving a smooth bend in the medial axis to the right of center.

Fourth row The same thing is happening now to left of center. By the end of the fourth row the medial axis has become a smooth U shape once both branches of the symmetry set have drifted clear. Note that the nearly vertical line outside the curve is also part of the medial axis but we have been concentrating on the interior part here.

5 Discussion

The first contribution of this paper is to formally classify the types of MA and SH points to support a directed planar graph representation of shape. This theoretical result can be viewed as a formal proof of the shock grammar proposed in [17]. It has in addition identified the ‘sources’ and ‘sinks’ of shock flow which are used to show formal correctness of an exact and near optimal flow-based shock recovery scheme proposed in [20]. This algorithm combines traditional curve evolution and computational geometry ideas by using the former to identify the sources and the latter to propagate shocks and the results presented in this paper are required the proof correctness of algorithm [19].

Second, in a recognition framework that is based on such skeletal representations, the similarity of two shapes, *e.g.*, the two fish in Figure 3(bottom), must remain stable across the instabilities of this representation. The second contribution of this paper is the formal derivation of the six instabilities depicted in Figure 20 which occur frequently in practice. The classification of these stabilities has allowed the derivation of a complete set of “edits” in an edit distance approach developed in [21, 12, 14], where each of the two distinct representations near the unstable (transition) skeleton are identified with the transitional skeleton itself, *i.e.*, the approach deforms both fish in Figure 3 by contracting the small segment between branches to more ‘symmetric’ ones where the two branches go through the same point (central column of Figure 20).

Acknowledgments

This material is based upon work supported by the National Science Foundation under Grants 0083231 and BCS-9980091. Any opinions, findings, and conclusions or recommendations expressed in this material are those of the author(s) and do not necessarily reflect the views of the National Science Foundation.

References

- [1] H. Asada and M. Brady. The curvature primal sketch. *IEEE PAMI*, 8:2–14, 1983.
- [2] H. Blum. Biological shape and visual science. *J. Theor. Biol.*, 38:205–287, 1973.
- [3] I. A. Bogaevsky. Metamorphoses of singularities of minimum functions, and bifurcations of shock waves of the Burgers Equation with vanishing viscosity. *St. Petersburg (Leningrad) Math. J.*, 1(4):807–823, 1990.
- [4] I. A. Bogaevsky. Perestroikas of shocks and singularities of minimum functions. April 2002. Pre-print, University of Liverpool/Independent University of Moscow.
- [5] J. Bruce and P. Giblin. *Curves and Singularities*. Cambridge University Press, 1984.
- [6] J. Bruce, P. Giblin, and C. Gibson. Symmetry sets. *Proceedings of the Royal Society of Edinburgh*, 101A:163–186, 1985.
- [7] J. W. Bruce and P. J. Giblin. Growth, motion and 1-parameter families of symmetry sets. *Proceedings of the Royal Society of Edinburgh*, 104A:179–204, 1986.

- [8] M. Buchner. The structure of the cutlocus in dimension less than or equal to six. *Compositio Mathematica*, 37:103–119, 1978.
- [9] D. Geiger, T.-L. Liu, and R. V. Kohn. Representation and self-similarity of shapes. In ICCV1998 [11].
- [10] P. J. Giblin and B. B. Kimia. On the intrinsic reconstruction of shape from its symmetries. In *Proceedings of the IEEE Computer Society Conference on Computer Vision and Pattern Recognition*, pages 79–84, Fort Collins, Colorado, USA, June 23-25 1999. IEEE Computer Society Press.
- [11] *Sixth International Conference on Computer Vision, Bombay, India, 1998*, Bombay, India, 1998. IEEE Computer Society Press.
- [12] P. Klein, S. Tirthapura, D. Sharvit, and B. Kimia. A tree-edit distance algorithm for comparing simple, closed shapes. In *Tenth Annual ACM-SIAM Symposium on Discrete Algorithms (SODA)*, pages 696–704, San Francisco, California, January 9-11 2000.
- [13] M. Leyton. Symmetry-curvature duality. *Computer Vision, Graphics, and Image processing*, 38:327–341, 1987.
- [14] T. Sebastian, P. Klein, and B. Kimia. An edit distance approach to shape matching. Technical Report LEMS 183, LEMS, Brown University, June 2000.
- [15] T. B. Sebastian, P. N. Klein, and B. B. Kimia. Recognition of shapes by editing shock graphs. In *Proceedings of the Eighth International Conference on Computer Vision*, pages 755–762, Vancouver, Canada, July 9-12 2001. IEEE Computer Society Press.
- [16] D. Sharvit, J. Chan, H. Tek, and B. B. Kimia. Symmetry-based indexing of image databases. *Journal of Visual Communication and Image Representation*, 9(4):366–380, December 1998.
- [17] K. Siddiqi and B. B. Kimia. A shock grammar for recognition. In *Proceedings of the Conference on Computer Vision and Pattern Recognition*, pages 507–513, 1996.
- [18] K. Siddiqi, A. Shokoufandeh, S. Dickinson, and S. Zucker. Shock graphs and shape matching. In ICCV1998 [11], pages 222–229.
- [19] H. Tek and B. B. Kimia. A discrete wave propagation method for the exact recovery of bisectors as shocks. Technical Report LEMS 181, LEMS, Brown University, December 1999.
- [20] H. Tek and B. B. Kimia. Symmetry maps of free-form curve segments via wave propagation. In *Proceedings of the Fifth International Conference on Computer Vision*, pages 362–369, Kerkyra, Greece, September 20-25 1999. IEEE Computer Society Press.
- [21] S. Tirthapura, D. Sharvit, P. Klein, and B. B. Kimia. Indexing based on edit-distance matching of shape graphs. In *SPIE Inter. Symposium on Voice, Video, and Data Communications, Boston*, pages 25–36, November 1998.
- [22] Y. Yomdin. On the local structure of a generic central set. *Compositio Mathematica*, 43:225–238, 1981.

- [23] S. C. Zhu and A. L. Yuille. FORMS: A flexible object recognition and modeling system. *Intl. J. of Computer Vision*, 20(3):187–212, 1996.